

X-Ray Imaging of Transient Cavitation Motion in Nozzles under Steady Injection Condition

¹Rubby Prasetya*; ¹Takashi Miwa; ¹Akira Sou; ²Seoksu Moon;
³Yoshitaka Wada; ³Yoshiharu Ueki; ³Hideaki Yokohata

¹Kobe University, Kobe, JPN; ²AIST, Tsukuba, JPN; ²Mazda Motor Corporation, Hiroshima, JPN

Abstract

High-speed X-Ray Phase Contrast Imaging (XPCI) was utilized to obtain a clear image of cavitation in two-dimensional (2D) nozzles with various sizes. The nozzles have variable widths W of 0.5, 1.0, and 2.0 mm. The length-to-width ratio of all nozzles are the same, $L/W = 4$. Injection was conducted under steady flow rate condition at two different flow rates to simulate incipient cavitation and super cavitation (the state where cavitation length extends until it almost reaches the nozzle exit). The results revealed that turbulence plays a large role in the bubble growth and shrink process in a nozzle. Cavitation film at super cavitation regime was observed to be comprised of more than a single cavitation film. Shedding of cavitation clouds from the tail end of the cavitation film near the side wall of the nozzle, where turbulence is very strong, was also observed.

Keywords: Nozzle internal flow; 2D nozzles; X-ray; XPCI

Introduction

In recent decades, various flow visualization methods utilizing x-ray as the light source have been increasingly used in the studies of optically dense multiphase flows [1], as it enables the visualization of optically dense areas without obstruction of multiple scattering. Within various x-ray visualization techniques, X-ray Phase Contrast Imaging (XPCI) is able to clearly differentiate objects with different densities, such as bubbles and drops. In the current study, propagation-based XPCI was utilized to obtain high-speed images of cavitation in symmetrical two-dimensional (2D) nozzles with various sizes, under steady injection condition.

Experimental Setup

The experiment were carried out at SPring-8 synchrotron radiation facility. XPCI experimental setup is shown in Figure 1(a), which is similar to those used in the authors' previous studies [2,3]. Filtered tap water at room temperature was injected into ambient air at a constant flow rate, through a 2D nozzle mounted in a test chamber. The 2D nozzles were comprised of aluminum or stainless steel plates, which were held between two acrylic plates. X-ray beam with approximately 0.5 mm in diameter at C-mode filling pattern as illustrated in Figure 1(b) was used in the experiment. The x-ray beam was converted by a Lu–Si–O scintillator crystal into a visible light with a wavelength of around 420 nm. The resulting light was then captured by a high-speed CMOS camera (Photron, SA-Z) with 2.1 $\mu\text{m}/\text{pix}$ in spatial resolution. Injection was conducted with two different mean velocities V in the nozzle to simulate incipient and super cavitation regimes. Detailed nozzle dimensions and flow velocities are shown in Table 1.

Nozzle Length L [mm]	Nozzle width W [mm]	L/W [-]	Nozzle inlet roundness R [μm]	R/W [%]	Nozzle thickness T [mm]	Nozzle Material	Velocity in nozzle V [m/s]	
							Incipient Cavitation	Super Cavitation
8.0	2.0	4	20.0	1.0	0.5	Stainless Steel	13.0	16.3
4.0	1.0		22.6	2.3		Aluminum	12.0	14.3
2.0	0.50		31.2	6.2		Aluminum	14.7	15.3

Table 1 Nozzle dimension and injection flow rate

*Corresponding Author, Rubby Prasetya: 142w601w@stu.kobe-u.ac.jp

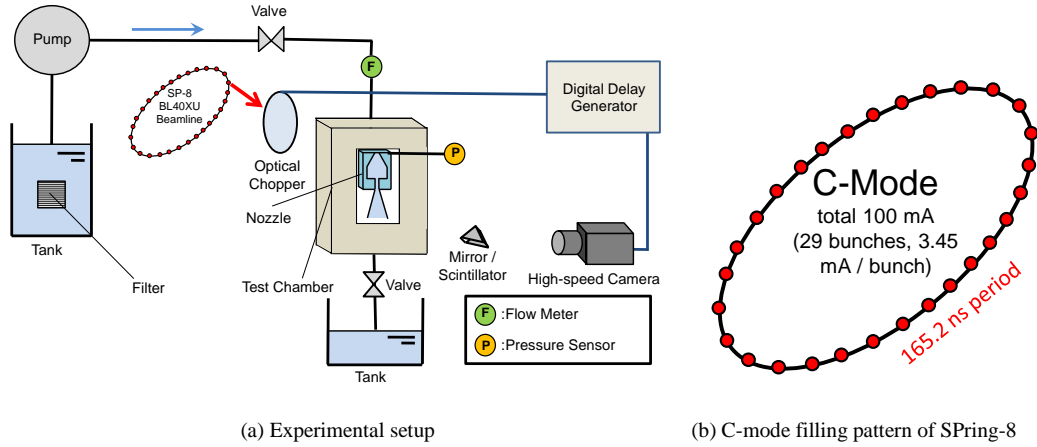


Figure 1 High-speed XPCI experimental setup

Results and Discussion

Representative images of incipient cavitation are shown in Figure 2. All images were taken near the nozzle inlet, with the position shown by a red rectangle in Figure 2. It was confirmed almost all incipient cavitation bubbles have non-spherical shapes. The bubbles tend to slant and elongate in the streamwise direction before they shrink and collapse. The slant and elongated shape of the bubbles is caused by the velocity profile of the recirculation flow, where the highest downward velocity appears near the outer edge of the boundary layer and an upward flow along the side wall [4]. Counter-clockwise rotational motion of bubbles near the side wall of the nozzle can be observed from Figure 2. The rotational motion is caused by the anti-clockwise eddies appearing along the outer edge of the boundary layer, near the reattachment point, and vortex shed from the point. These observations confirm that there is a strong relation between turbulent flow and cavitation in the nozzle.

To investigate the bubble growth and shrink process, equivalent diameter D_e of each cavitation bubble that was highlighted in Figure 2(a–c) was measured for each nozzle, where D_e is given by Equation (1):

$$D_e = \frac{2(X_{cv}X_{ch})}{(X_{cv}+X_{ch})} \quad (1)$$

where X_{cv} is the vertical chord length and X_{ch} is the horizontal chord length of a given bubble. The measurement result is summarized in Figure 3.

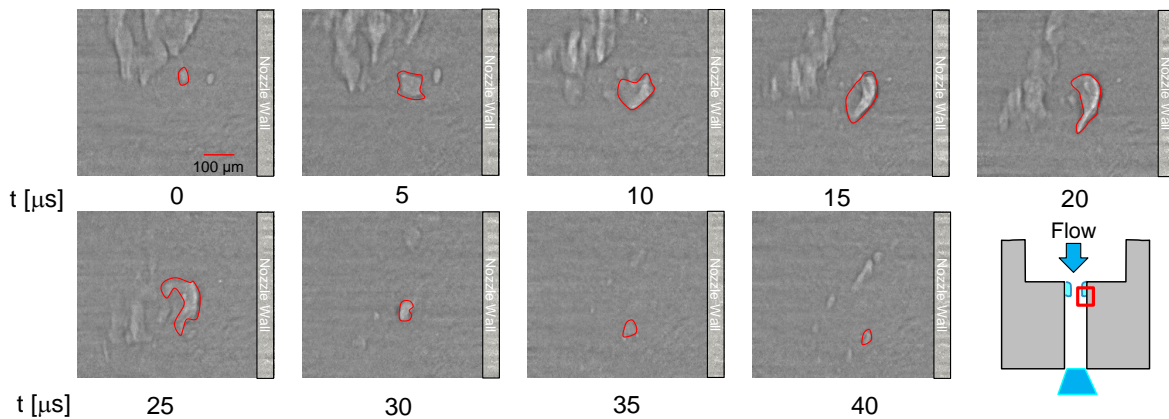


Figure 2(a) Incipient cavitation in nozzle with $W = 2.0$ mm and $V = 13.0$ m/s

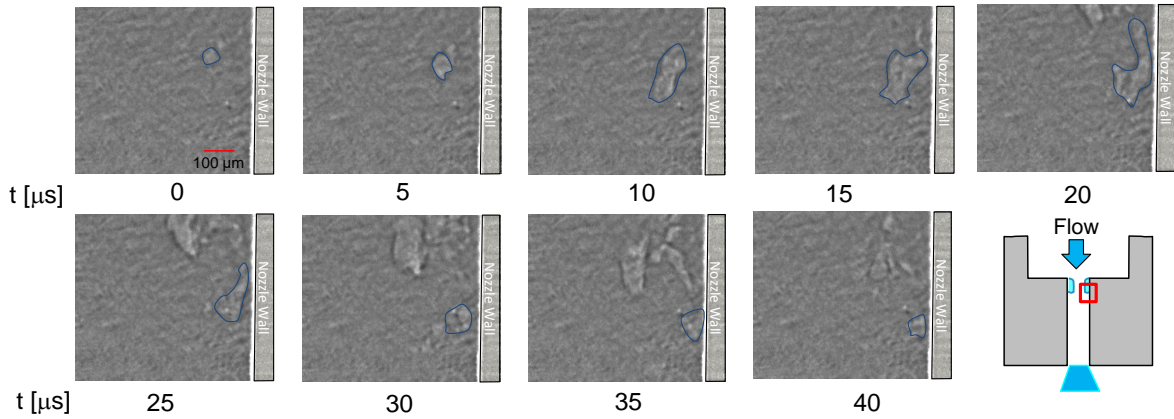


Figure 2(b) Incipient cavitation in nozzle with $W = 1.0$ mm and $V = 12.0$ m/s

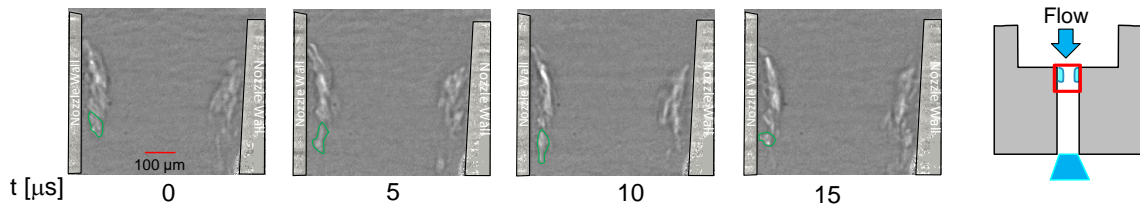


Figure 2(c) Incipient cavitation in nozzle with $W = 0.50$ mm and $V = 14.7$ m/s

Figure 3 shows the changes in incipient cavitation bubble size for each nozzles. The difference in bubble size for each nozzles are caused by the similarity law, that is, the diameters of incipient cavitation bubbles scales proportionally to the nozzle size [3]. It should be noted that as Figure 3 only serves to illustrate the growth and shrink process of a typical cavitation bubble in nozzles with different sizes. As Figure 3 only shows the diameter of a single bubble for each nozzles, the bubble size shown in Figure 3 should not be taken as a representative bubble size.

From Figure 3, it can be seen that while it takes about 10-20 μs for a bubble to grow, the shrink of a bubble happens within much shorter period, about 5 μs . The time scale of the bubble growth and shrink process simply estimated by the Rayleigh-Plesset equation is much shorter from those observed in the present study, which suggests the fact that the process is governed by turbulent flow in the nozzle.

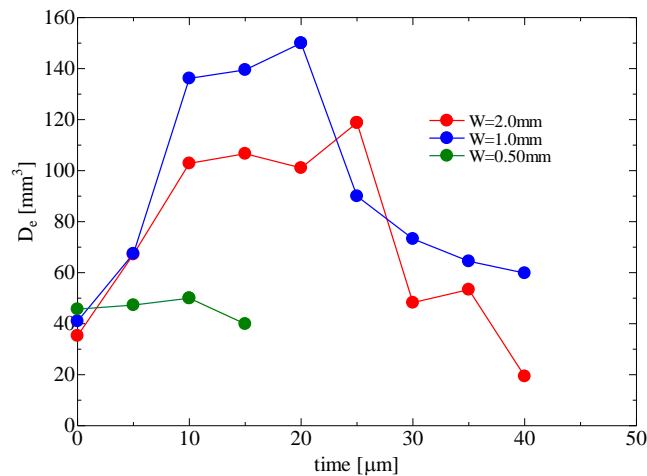


Figure 3 Time histories of equivalent bubble diameter D_e during growth and shrink process

Images of region near the tail end of a cavitation film at super cavitation regime for the nozzle with $W = 1.0$ mm is shown in Figure 4. The super cavitation film in the 2D nozzle consists of two cavitation films, which can be caused by the surface roughness of the nozzle inlet edge whose thickness is 0.5 mm. Another thing that is observable from Figure 4 is the formation and shedding of cavitation bubble clouds from the tail of the super cavitation film near the side wall, where the reattachment of the separated flow and the shedding of vortex take place and strong turbulence is generated.

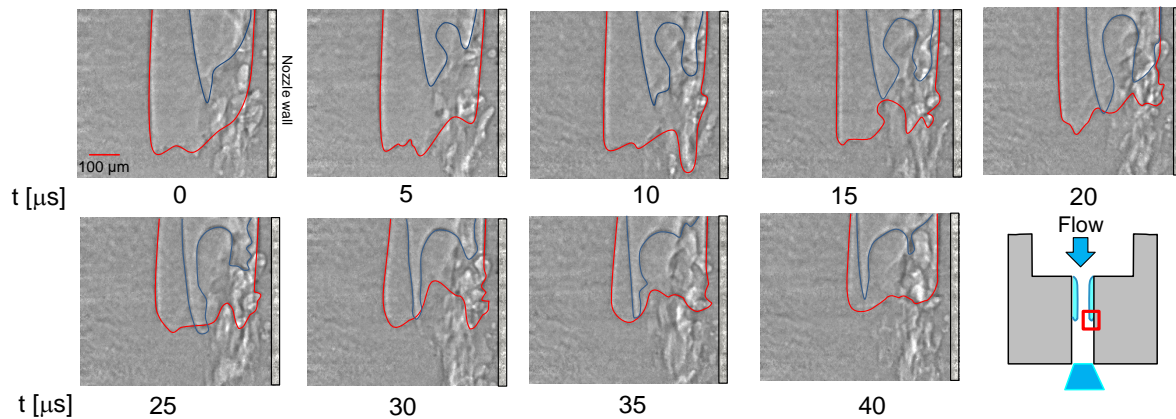


Figure 4 Tail of super cavitation in nozzle with $W = 1.0$ mm

Conclusion

XPCI experiment was conducted to visualize cavitation in symmetrical 2D nozzles with various sizes. The results revealed that incipient cavitation bubbles have deformed, non-spherical shapes. The incipient cavitation bubbles grow and elongate following the recirculation flow in the nozzle, while rotating in counter-clockwise direction following the eddies near the right wall of the nozzle, before the bubbles shrink and collapse in the shed vortex. Cavitation film at super cavitation regime was observed to be comprised of two cavitation films, which was probably caused by uneven surface roughness along the inlet edge of the nozzle. Cavitation clouds were shed from the tail of the cavitation film, where reattachment of the separated flow vortex shedding generates strong turbulence. These observations confirm the fact that turbulence and flow structure play an important role in cavitation in the nozzle.

Acknowledgments

Synchrotron radiation experiment was performed at the BL40XU beamline of SPring-8 with the approval of Japan Synchrotron Radiation Research Institute (JASRI) (Proposal No. 2015B0111). The authors would like to extend their gratitude to the SPring-8 beamline scientist Nobihuro Yasuda his technical assistance during the experiment.

References

- [1] Heindel, T.J. (2011). *A Review of X-Ray Flow Visualization With Applications to Multiphase Flows*. J Fluids Eng 133(7).
- [2] Moon, S., Komada, K., Sato, K., Yokohata, H., Wada, Y., Yasuda, N. (2015). *Ultrafast X-ray study of multi-hole GDI injector sprays: Effects of nozzle hole length and number on initial spray formation*. Exp Therm Fluid Sci 68.
- [3] Sou, A., Minami, S., Prasetya, R., Pratama, R.H., Moon, S., Wada, Y., Yokohata, H. (2015). *X-Ray Visualization of Cavitation in Nozzles with Various Sizes*. Proceedings of The 13th International Conference on Liquid Atomization and Spray Systems - ICLASS 2015, Tainan, Taiwan.
- [4] Sou, A., Hosokawa, S., Tomiyama, A. (2006). *Effects of cavitation in a nozzle on liquid jet atomization*. Int J Heat Mass Transf. 50(17-18).